

SPECTROPHOTOMETRY OF M33 CLUSTERS

C. A. CHRISTIAN¹

Institute for Astronomy; and Canada-France-Hawaii Telescope Corporation, Kamuela, Hawaii

AND

R. A. SCHOMMER¹

Rutgers University, Piscataway, New Jersey

Received 1983 February 28; accepted 1983 May 12

ABSTRACT

Intermediate-resolution spectrophotometry (10 Å) obtained for 20 M33 clusters was compared with similar data for M31, LMC, and SMC clusters. The existence of clusters with a range of properties (age, metallicity, integrated spectral types) has been verified. The M33 clusters span a range of ages from 10^7 to 10^{10} yr. The range of metallicities ($-2.0 < [\text{Fe}/\text{H}] < 0.0$) is roughly correlated with the age ranking derived from the integrated spectral types. The reddest clusters exhibit properties similar to Galactic globular clusters; none of the clusters appear to be as metal-poor as M15 or as metal-rich as the strong-lined clusters found in M31.

Subject headings: clusters: globular — galaxies: individual — spectrophotometry

I. INTRODUCTION

Detailed studies of globular clusters, practical only for Local Group galaxies (cf. Harris and Racine 1979), have indicated that old, red, relatively metal-poor globular clusters can be found in the Galaxy, M31, and the Magellanic Clouds. In addition, large numbers of "populous," young, blue clusters have been found in the LMC and the SMC but not in the Galaxy or M31. The system of clusters in M33 is potentially interesting because this small Sc galaxy represents a morphological type intermediate between the large "early-type" spiral galaxies and the dwarf irregular galaxies in the Local Group.

As shown by Christian and Schommer (1982, hereafter Paper I), the number of "classical" red globular clusters is at least 13, whereas previous estimates (Hiltner 1960; Kron and Mayall 1960) suggested that M33 contained only a few (< 5) such objects. In addition, a number of luminous ($M_v < -6$) blue and intermediate-color objects were found. In Paper I, it was suggested that the blue nonstellar objects found in the M33 field are clusters analogous to the populous clusters recently formed in the Magellanic Clouds. The intermediate-color objects, $0.3 < B - V < 0.6$, are alleged to be well-populated intermediate-age clusters, i.e., extremely massive versions of LMC clusters NGC 2209 and NGC 1868.

The verification of the cluster identities has ramifications for galactic evolution theories in that it appears that M33 may have had a smoother star formation rate than any other Local Group galaxy studied thus far. Intermediate-resolution (~ 10 Å) spectrophotometry

can be used not only to estimate cluster ages via integrated spectral types, but also to study the abundances and kinematic properties of the clusters in the system. The observations employed to this end are described in § II, the integrated spectral types are presented in § III, and a discussion of metallicity estimates, in reference to age estimates and galactic evolution theories, is presented in § IV. The subject of the kinematics of the cluster system will be published separately.

II. OBSERVATIONS AND REDUCTIONS

In 1981 November and 1982 September, the intensified image dissector scanner (IIDS) was used on the 4 m telescope at the Kitt Peak National Observatory (KPNO) to obtain spectrophotometry of the M33 clusters covering the spectral region 3700–5500 Å. Grating #26 (600 lines mm^{-1}) was implemented with aperture #6 (4.4 diameter) to give a resolution of 9.5 Å. A number of "IIDS standard" stars (Strom 1977) and several comparison stars were observed each night. The standard stars were used to transform the observations into fluxes during the reduction process, while the comparison stars were used as fiducial objects for the integrated spectral types and metallicity estimates. All observations were processed with the (improved) reduction procedures, which have been documented thoroughly elsewhere (cf. Christian 1981; McClure and Hesser 1981).

III. INTEGRATED SPECTRAL TYPES AND CLUSTER AGES

Integrated spectral types were estimated by visual examination of the cluster spectra in order to investigate the range of cluster ages represented. Comparison objects observed include stars in NGC 2158, M15, M31, and a selection of stars measured by Suntzeff (1980)

¹ Visiting Astronomer, Kitt Peak National Observatory, operated by Associated Universities for Research in Astronomy, Inc., under contract with the National Science Foundation.

M33 CLUSTERS

 TABLE 1
 INTEGRATED SPECTRAL TYPES AND PHOTOMETRY OF M33 CLUSTERS

Object	Sp. T.	V	$B-V$	Age Class ^a	Comment
U62.....	A1	16.55	0.12	Y	
U148 ^b	A1	...	0.15	Y	
M4.....	A2	16.64	0.21	Y	
M6.....	A2	16.48	0.21	Y	+ O stars
U79.....	A1	17.48	0.26	Y	
Cl 27.....	A3-5	17.19	0.37	Y	λ 5007 [O III] emission
U101.....	A2	17.69	0.42	Y-I	
U83.....	A9	17.66	0.49	Y-I	
U105.....	H II	17.75	0.52	Y	
Cl 39.....	F3	15.91	0.56	I	
H II 21.....	F5	17.46	0.61	I-O	
U77.....	F?	17.19	0.67		Poor signal-to-noise ratio
U49.....	F8	16.25	0.68	I-O	
R14 ^{b,c}	G0	...	0.68	O	
M9.....	F8	17.06	0.72	I-O	
Cl 18.....	G1	18.16	0.73	O	
Cl 38.....	F5	18.10	0.73	I-O	
Cl 20.....	F8-G0	17.67	0.77	O	
R12 ^{b,c}	G3	...	0.77	O	
H II 38.....	G2	17.24	0.83	O	
Cl 26.....	F8	18.00	0.88	I-O	

^a Y = age < 10⁸, I = age ~ 10⁹, and O = age > 10¹⁰.

^b Colors estimated from IIDS spectrophotometry.

^c R12 and R14 identified by R. Racine on CFHT 3.6 m prime-focus plate (15 minute exposure, IIA-O, seeing 0".5).

and Burstein *et al.* (1982, hereafter BFGK). Additional comparison objects derived from a grid of stars with the same instrumentation on the KPNO 2.1 m telescope for separate programs by Christian and Smith (1983) and Christian (1981). The spectral type of an individual star which most closely resembled the spectrum of each cluster is listed in Table 1, along with integrated photometry from Paper I. Obviously, the integrated cluster spectra do not perfectly match the spectrum of any single star, but the spectral types do serve to rank order the spectra in a self-consistent way. The spectra of the M33 and M31 clusters in our program are shown in Figures 1a-1f, in order of increasing ($B-V$). The spectrum of U105 [$(B-V) = 0.54$] has been omitted as this object is an H II region.

The integrated spectral types clearly correlate with the integrated photometry, which establishes the identity of the blue and intermediate-color objects as young and intermediate-age clusters. In particular, it is seen that intermediate-color objects indeed have intermediate integrated spectral types rather than being young clusters embedded in obscuring (reddening) material. It was anticipated in Paper I that these clusters were not likely to exhibit substantial reddening because they are located well outside the dusty patches seen in the M33 disk. However, the existence of bright, intermediate-color clusters is unprecedented in studies of other Local Group galaxies, so verification of cluster ages from the integrated types was a key point in the analysis.

Table 1 also lists preliminary age classifications for the clusters, based on a comparison of the IIDS spectra of the M33 clusters with the spectra of LMC clusters, M31 clusters, and Galactic globular clusters (Rabin 1982; S. Faber, private communication; H. A. Smith and L. Searle, private communication) and Cohen's (1982) age scale. Rabin has described the pitfalls of estimating cluster ages without independent abundance measurements; the arguments will not be repeated here. The ages listed in this table were used merely as a springboard for the ensuing discussion.

IV. NARROW-BAND INDICES

The range in cluster spectral types (and therefore ages) suggests that the star formation rate might have been relatively constant in M33, while it could be that star formation in the Galaxy (and to a lesser extent in the LMC) occurs in bursts (Rabin 1982; Aaronson and Mould 1982). The environments in the M33 halo and disk apparently are conducive to the continual production of well-populated clusters. In the Galaxy, the production of massive clusters once occurred in the halo but seems to have ceased, so far as we can ascertain. In the LMC, the production of populous clusters appears to have been sporadic, more recent, and longer lived (Rabin 1981; Aaronson and Mould 1982).

To study the cluster ages and abundances, narrow-band indices were simulated by taking into consideration the work of O'Connell (1982), Suntzeff (1980), Kinman,

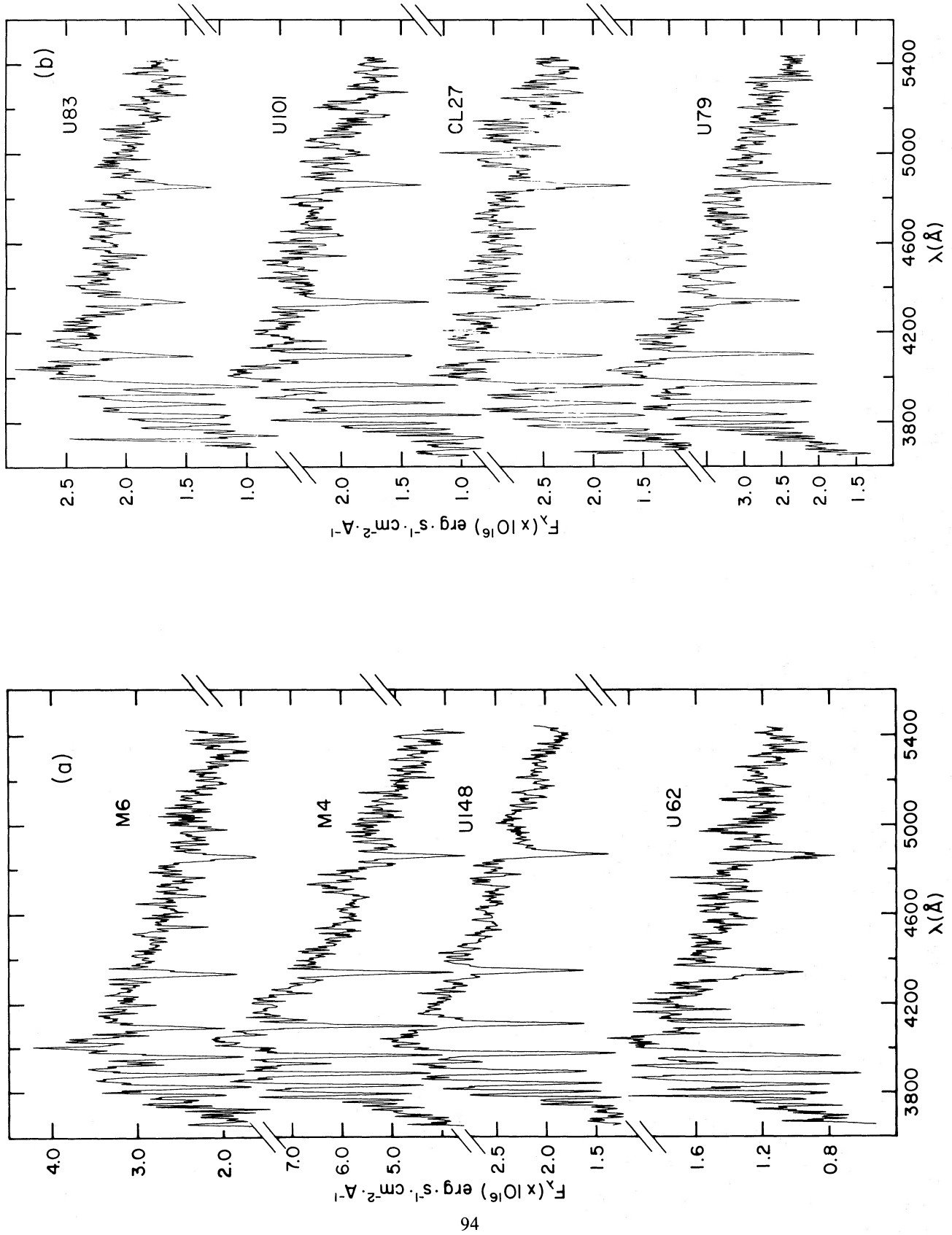


FIG. 1.—IIDS scans of M33 and M31 clusters arranged in order of increasing $(B - V)$

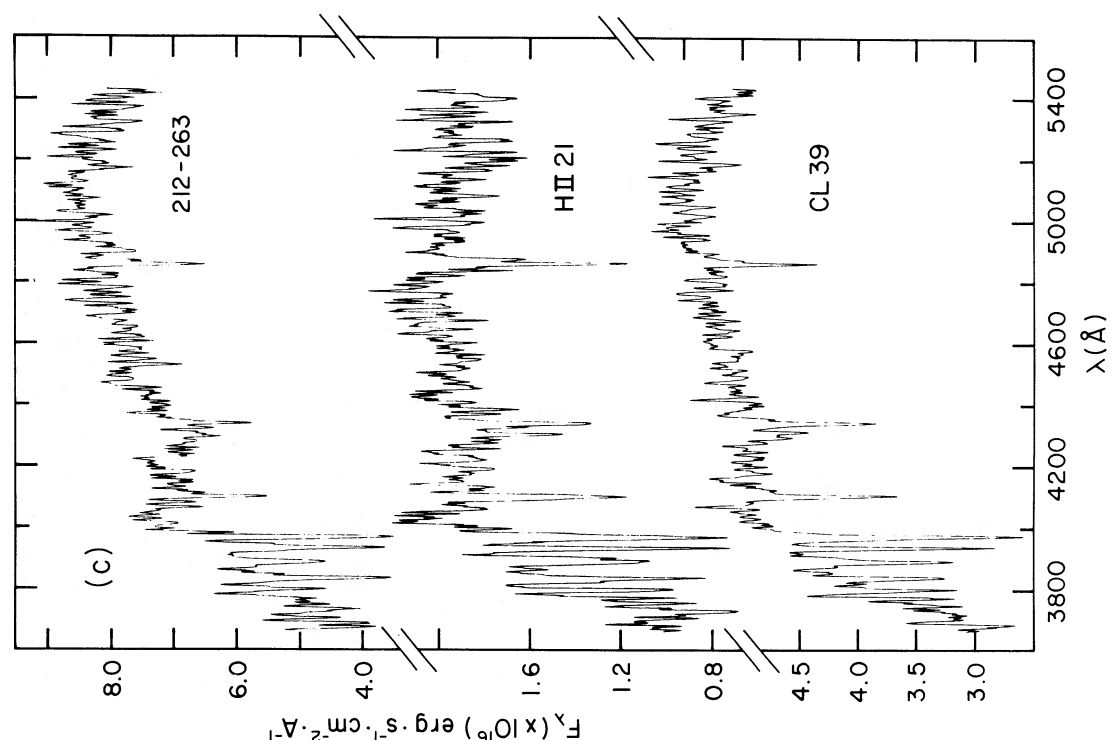
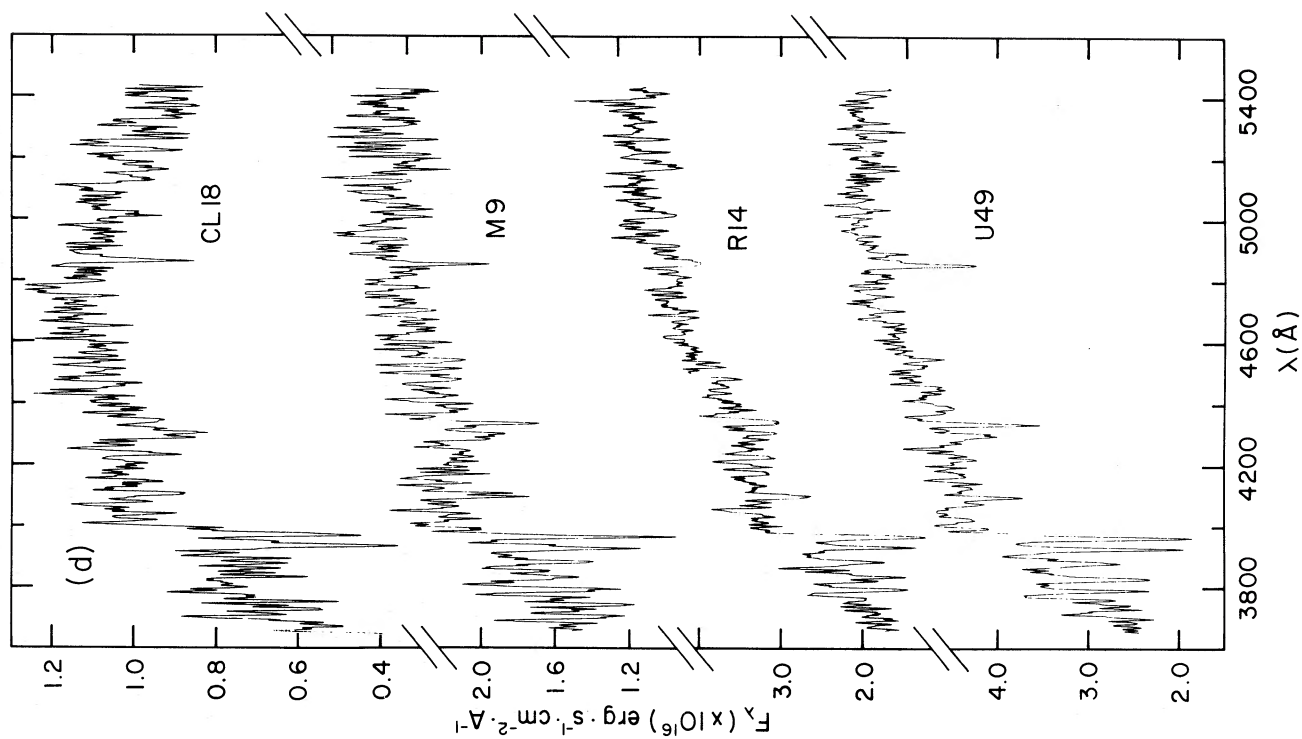


Fig. 1—Continued

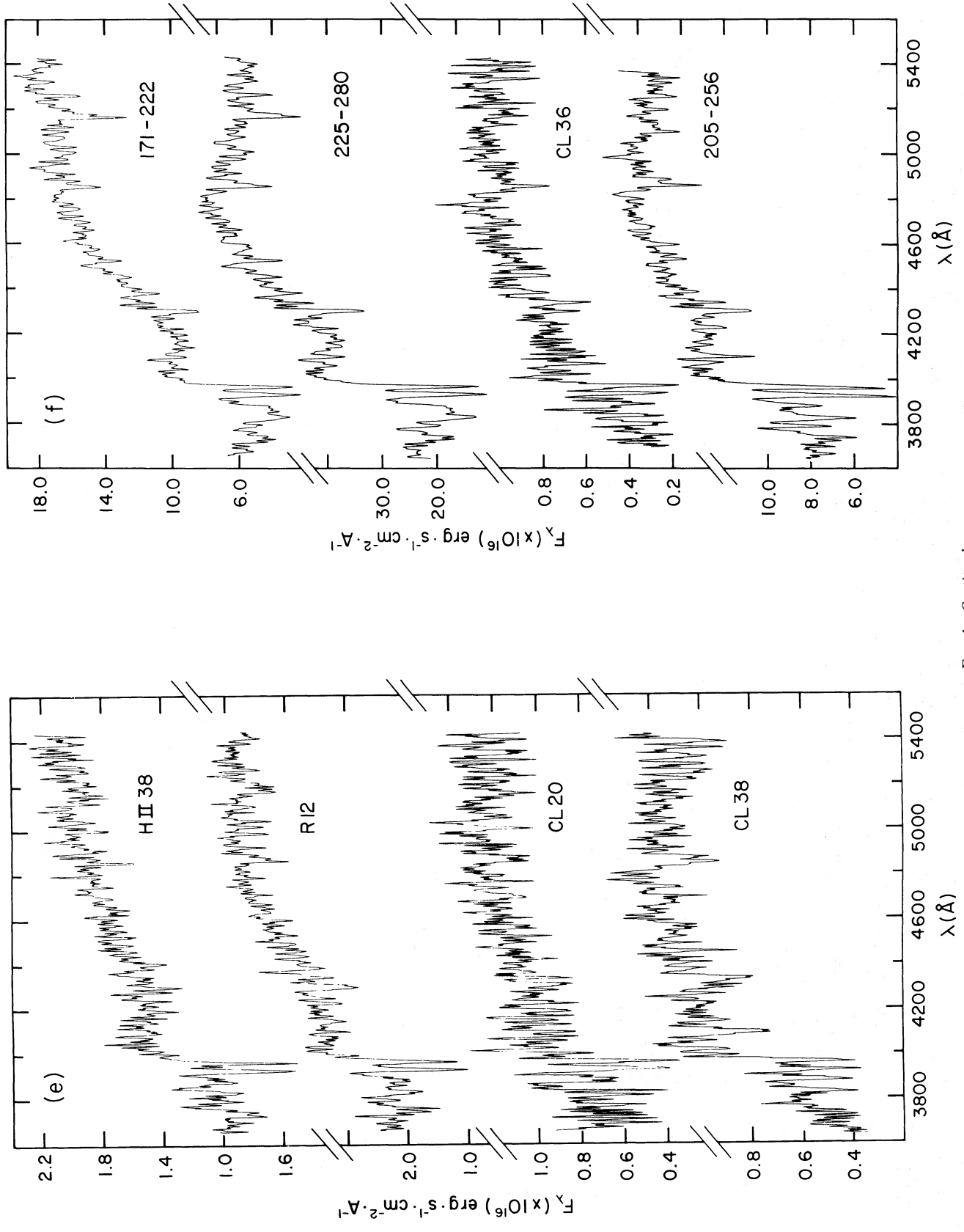


FIG. 1—Continued

TABLE 2
NARROW-BAND INDICES SIMULATED FROM IIDS DATA

Index	Feature	Ref.	Standards
H β	W_{eq} H β	1	HR 1805, HR 2002, HR 2600, M15, M31 212-263, M31 171-222
Mg II	Mg λ 5175	1	HR 1805, HR 2002, HR 2600, M15, M31 212-263, M31 171-222
m_{HK}	Ca II H, K	2	M15, M3, HD 2265, HD 88609
CN λ 4170	CN λ 4216 band	1	M15, M3, M31 212-263, M31 171-222

REFERENCES.—(1) BFGK (see text). (2) Kinman, Kraft, and Suntzeff 1981.

Kraft, and Suntzeff (1981), Rabin (1982), and BFGK, who measured features such as the Ca H and K lines, Balmer absorption, CN, and Mg absorption in the spectra of individual stars and globular clusters in the Galaxy, M31, and the MC. In the subsequent discussion, narrow-band indices calculated from stellar spectra are used to estimate the cluster ages and metallicity scale, but we regarded a detailed deconvolution of the spectra well beyond the scope of this discussion. The cluster parameters thus derived are to be regarded with caution; clearly, the spectrum of an individual star does not totally reproduce the features of any integrated cluster spectrum.

The narrow-band indices used to investigate the M33 clusters are described in Table 2. “Standard” stars were observed either with the 2.1 m telescope or the 4 m telescope to establish transformation relations from the simulated indices to the published scales. Although the transformations were performed to facilitate comparison of our data with a variety of other studies, it should be noted that the IIDS data comprise a self-consistent set which can be evaluated independently of the published studies. That is, the relative metallicity and age scales derived herein are not affected by the details of the transformation equations, described below. The calculated indices are listed in Table 3, where the following notation was adopted for the M31 clusters: the designation 212-263, for example, refers to the cluster numbers 212 and 263 in the catalogs of Battistini *et al.* (1980) and Sargent *et al.* (1977), respectively.

Our H β , CN λ 4170, and Mg II indices correspond directly to the values measured by BFGK, except for a slight zero-point shift which was applied to the Mg II index. Based on observations of six objects, the rms agreement for the Mg II index is remarkably good, 0.02. The H β equivalent widths agree with BFGK values to within +0.39 Å (rms). We do not have good comparative values for CN λ 4170, but examination of BFGK’s Figure 3 suggests the rms differences are similar to the Mg II scale.

Our m_{HK} index was transformed to Kinman, Kraft, and Suntzeff’s (1981) scale using

$$m_{\text{HK}} = 1.25m_{\text{HK}}(\text{observed}) - 0.63 \quad (\pm 0.04).$$

The slope of this relation differs from unity most likely as a result of the difficulty often encountered when converting intermediate-resolution observations to flux measurements. Problems can arise from two sources: First, if few flux points are available for standard stars, spurious fluctuations between the flux points can be introduced by the fitting routine, especially if polynomial relations are used. Second, the presence of strong absorption features in this particular wavelength region (3400–4000 Å) inhibits the usefulness of both the “standard” values and the spectrophotometric observations. In F–G stars this problem is severe because of the presence of the Ca II H and K lines and Balmer absorption. Most of the flux standards used in this program were subdwarfs and early-type stars, so much of the discrepancy between our measurements and the published m_{HK} scale probably arose from the differences in the particular flux points and fitting routines used.

Comparison of data for individual objects measured on several nights showed that the repeatability of the measurements is on the order of or better than the rms values quoted above. The measurement errors for objects with poorer signal-to-noise ratios—for example, CL 20—are slightly worse.

Finally, synthetic “IIDS-type” scans of A–G stars were simulated using Kurucz’s models (Kurucz 1979) by linearly interpolating between the published flux points to produce spectra similar to those observed. The models included T_{eff} from 5500 to 8500 K, $\log g = 4$, and $[\text{Fe}/\text{H}] = 0.0, -1.0, \text{ and } -2.0$, as well as a few models with lower $\log g$, representing higher luminosity stars. Line indices were computed for the synthetic scans and converted to the published scales in the same way as the observed data. The indices from the models were compared with the observed indices for stars of similar type, or to published synthetic photometry (e.g., Gustafsson and Bell 1978), with the result that the H β indices were recomputed, using a much wider bandpass than used by BFGK. The interpolation procedure tends to widen absorption features artificially, but only the H β index appeared to be affected significantly. With these caveats, the “model indices” were used to supplement the grid of comparison indices in the following analysis.

TABLE 3
INDICES COMPUTED FROM IIDS SPECTROPHOTOMETRY

Object	H β	Mg II	m_{HK}	CN λ 4170	log (age) ^a
M33 and M31 Clusters					
U62	8.12	0.034	0.41	-0.20	7.2
U148	6.98	0.050	0.42	-0.29	7.7
Cl 27	6.32	0.093	0.41	-0.29	7.9
U79	6.25	0.006	0.46	-0.29	8.0
M6	6.17	0.029	0.51	-0.11	8.0
U101	5.99	0.106	0.40	-0.22	8.1
M4	5.93	0.029	0.51	-0.12	8.1
U83	5.37	0.108	0.63	-0.23	8.3
H II 21	4.82	0.083	0.64	-0.21	8.5
Cl 18	3.07	0.039	0.94	-0.11	9.3
212-263	2.83	0.019	0.72	-0.11	9.3
U49	2.73	0.068	0.74	-0.09	9.4
Cl 39	2.57	0.024	0.63	-0.11	9.5
Cl 36	2.39	0.132	0.71	-0.02	9.5
Cl 38	2.06	0.019	0.83	-0.13	>9.6
225-80	2.05	0.156	1.02	+0.04	>9.6
M9	2.03	0.093	0.72	-0.12	>9.6
R14	1.86	0.086	0.78	-0.11	>9.6
R12	1.82	0.154	0.92	-0.01	>9.6
H II 38	1.72	0.107	0.88	-0.05	>9.6
205-256	1.71	0.089	0.89	-0.09	>9.6
171-222	1.57	0.228	0.98	+0.05	>9.6
Cl 20	1.07	0.092	0.81	-0.09	>9.6
M15					
I-38	1.16	0.044	0.79	-0.05	...
II-54	1.81	0.021	0.68	-0.08	...
P8	1.39	0.006	0.77	+0.03	...
S1	1.07	0.026	0.92	-0.03	...
S4	1.16	0.022	0.95	+0.06	...
S6	0.73	0.050	0.97	-0.04	...
S36	1.19	0.024	0.77	-0.05	...
NGC 2158					
1-5-13	1.62	0.452	0.96	+0.12	...
3-4-1	1.36	0.204	1.22	+0.09	...
4-4-13	0.98	0.129	1.16	+0.01	...
4-2-69	0.63	0.347	1.39	+0.14	...
C	4.25	0.057	0.69	-0.14	...
Field Stars					
HR 1322	3.24	0.094	0.95	-0.07	...
HR 1591	4.80	0.049	0.74	-0.11	...
HR 1805	0.84	0.361	1.24	+0.33	...
HR 2002	2.33	0.207	1.02	+0.19	...
HR 2600	1.70	0.237	1.26	+0.14	...
HR 6770	1.93	0.114	1.16	+0.13	...
HR 7429	0.83	0.318	1.16	+0.27	...
HR 7576	1.16	0.347	1.14	+0.48	...
HD 2265	1.80	0.039	0.89	-0.07	...
HD 88609	0.85	0.046	0.76	-0.06	...

^a Approximate ages based on H β strength (see text).

V. METALLICITIES AND AGES FROM NARROW-BAND INDICES

The indices, simulated from the IIDS data and converted to the standard scale, are compiled in Table 3

for objects observed in 1981–1982. The relative variations of indices were investigated in an attempt to identify the characteristics of the M33 clusters individually and collectively. First, the indices are studied in pairs, where at least one index is thought to be dominated by age or metallicity effects. In § Ve, we discuss the cumulative information gained from the analysis.

a) m_{HK} versus $(B-V)_0$

Figure 2 shows the variation of m_{HK} versus $(B-V)_0$, analogous to Figure 1 in Suntzeff's (1980) work on Galactic globular cluster stars. The integrated $(B-V)$ values for the clusters were not corrected for internal or foreground reddening. For example, the nominal $E(B-V)$ for M33 is ~ 0.06 mag (Paper I), so a correction would affect the appearance of Figure 2 slightly, but not enough to radically change the qualitative information derived from it. Also, unknown reddening internal to M33 could alter the position of a cluster a small but indeterminate amount.

In the figure, the dot-dashed line represents the loci of solar neighborhood dwarfs, observed in 1979 and 1980. For $(B-V) < 0.50$ mag, higher luminosity early-type stars scatter near and slightly below this line, as shown. The high-luminosity stars have weaker m_{HK} indices when compared with dwarfs with similar spectral types owing to the relative decrease in the hydrogen features at lower log g , which overwhelms the increase in the Ca II H and K lines. The locus of indices computed from the Kurucz models (log $g = 4$) are shown for $[\text{Fe}/\text{H}] = -1.0$ (dashed line) and $[\text{Fe}/\text{H}] = -2.0$ (dotted line); the models with $[\text{Fe}/\text{H}] = 0.0$ fall along the solar neighborhood line, as expected. The few indices computed from metal-poor models with lower log g tend to fall below the indicated sequences, as did the observed indices for solar-neighborhood high-luminosity stars. In general, then, these two indices are indicative of both the presence of luminous stars and abundance variations in blue clusters. That is, although there is some tendency for the M33 data to fall close to the metal-poor sequences (for which log $g = 4.0$), the importance of luminous stars in the integrated spectra also can cause the M33 clusters to have apparently weak m_{HK} indices at a given color for $(B-V) < 0.50$.

In the upper right portion of the figure, the loci of individual giant star sequences in M3, M15, and M92 are shown, as derived from our data and those measured by others (N. Suntzeff, R. Kraft, and E. Friel, private communication). It can be seen that stars of different metallicities can be rank ordered according to their position in this diagram, as described by Suntzeff (1980). Note, however, the apparent degeneracy of the system at high metallicities, $[\text{Fe}/\text{H}] > -1.2$ (also see McClure and Hesser 1981; Canerna, Harris, and Farrell 1982). Although integrated indices for clusters are not best represented by those for single stars, integrated cluster light which contains significant contributions in the blue from main-sequence and horizontal-branch stars should be represented by a point much lower and farther to the left than the individual giants, for example, M15.

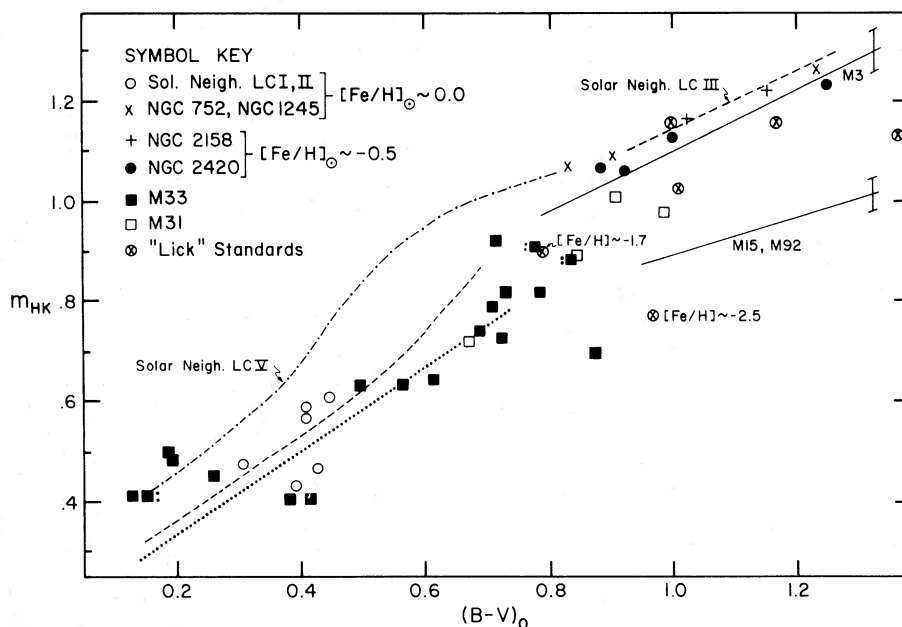


FIG. 2.—Index m_{HK} vs. $(B-V)$ for M33 clusters and comparison objects. The loci of solar-neighborhood stars are derived from IIDS observations accumulated in 1979–1980. The sequences of early-type stars were derived from synthetic IIDS scans computed from Kurucz's (1979) models of A–G stars. The loci of the M3, M15, and M92 sequences derive from IIDS data obtained by the authors, from Kinman, Kraft, and Suntzeff (1981), and from N. Suntzeff, R. Kraft, and E. Friel (private communication). "Lick" standards refer to standard stars observed in common with the above authors and BFGK. The error bars indicate the total scatter in the data along each sequence.

Thus, the figure does suggest that even the reddest M33 clusters are more metal-rich than M15 and M92. Note also the position of the M31 cluster 212–263, $(B-V) = 0.66$, which appears to be similar in many respects to intermediate-color M33 clusters. At the other extreme, the position of cluster 171–223, $(B-V) = 0.98$, is consistent with its spectral type, which resembles a more metal-rich K0 giant.

Basically, Figure 2 suggests the majority of M33 clusters describe a one-dimensional sequence spanning the region $0.12 < (B-V) < 1.0$ mag. Notable exceptions to the rule are the blue clusters Cl 27 and U101, which are located below and to the right of the sequence, and in the case of Cl 27, emission lines could contribute to a redder $(B-V)$ (cf. O III $\lambda 5007$ emission in Fig. 1). The cluster Cl 36 has an extremely red color but a spectrum more similar to U49 (F8). Cl 18 exhibits relatively strong H and K lines for its integrated $(B-V)$, which could be influenced by reddening and/or the presence of luminous red stars in the cluster.

b) $H\beta$ versus $Mg II$

BFGK have discussed the $H\beta$ versus $Mg II$ diagram (cf. Fig. 3) for globular clusters in the Galaxy and M31. The mean loci for these objects are shown as solid lines, and a few measurements of individual clusters, taken from BFGK, are shown for reference. This diagram is particularly germane to an analysis of the M33 data in that integrated spectra for a variety of stellar systems have been measured with this system.

The loci of the indices computed from the model A–G stellar spectra are shown in the upper portion of the

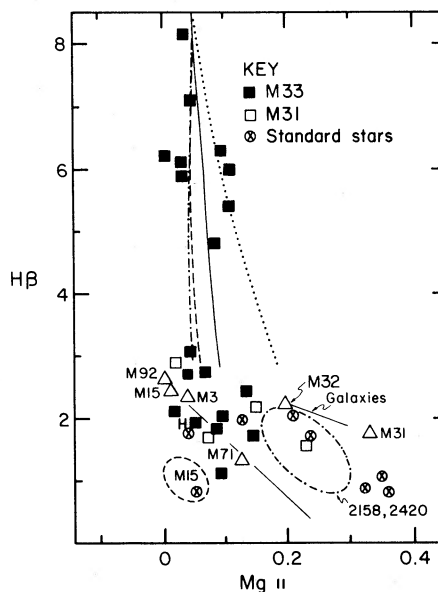


FIG. 3.— $H\beta$ vs. $Mg II$. Integrated indices from BFGK are shown as triangles, while data for individual stars in NGC 2158, NGC 2420, and M15 are enveloped by dot-dashed and dashed ellipses. The loci of data derived from models for $[Fe/H] = -2.0$, -1.0 , and 0.0 are shown as dot-dashed, dashed, and solid lines, respectively. Data for early-type solar-neighborhood stars of luminosity class V and I fall along the solid and dotted lines, respectively. The solid line in the lower portion of the figure joins the loci of Galactic globular clusters as shown in BFGK.

figure as solid, dashed, and dot-dashed lines for $[\text{Fe}/\text{H}] = 0.0, -1.0, -2.0$, respectively. Note the small scatter in the Mg II index for hot stars with similar T_{eff} but different $[\text{Fe}/\text{H}]$. Measured indices for individual stars are located near these lines except those for luminosity class I stars, which have luminosity-enhanced atomic lines near 5180 \AA , as indicated by the dotted line.

The positions of the indices measured for M15 giants are encircled by a dashed ellipse in the figure. The values for the integrated M15 spectrum, measured by BFGK, also are plotted. It is clear that the contribution to the integrated light in M15 due to blue horizontal-branch (BHB) stars enhances the $\text{H}\beta$ equivalent width but does not affect the Mg II index. This point is substantiated considering the position of the M15 BHB star, II-54, which is indicated by *H* in the figure. Thus, the Mg II index does appear to be a good indicator of cluster metallicity, at least for low-abundance objects; i.e., the presence of blue starlight in integrated cluster spectra does not severely weaken the Mg II index (as opposed to an $\text{Mg } b$ equivalent width).

At higher metallicities, the indices of galactic nuclei measured by BFGK appear to be consistent with this idea when compared with the positions of evolved stars in NGC 2158, NGC 2420, and solar-neighborhood giants. That is, the galactic nuclei exhibit excess $\text{H}\beta$ strength relative to the spectra of evolved stars, which are presumed to be representative of late-type stellar constituents of these objects (also see Gunn, Stryker, and Tinsley 1981; BFGK; and Boroson 1982). The data for M32 and M31 indicate the situation is more complex however, as these objects are believed to contain only relatively old populations (cf. Pritchett 1977; O'Connell 1982). Therefore, in some instances, it is the Mg II index which is enhanced, at a given value of $\text{H}\beta$, owing to high-metallicity stars. This may be relevant for clusters R12 and Cl 36; R12 has the largest Mg II index and is displaced from the metal-rich end of the Galactic globular cluster sequence in the direction of higher metallicity. Cl 36 is situated above the main distribution of M33 clusters, closer to M32 and the M31 cluster 171-223, and as mentioned above, this cluster has a spectral type $\sim \text{F8}$ but an extremely red $(B-V)$. In fact, the M33 clusters exhibit a small range in Mg II , in contrast to M31 clusters and galactic nuclei, suggesting that none of these clusters contains extremely metal-rich evolved stars, and many of the red clusters—for example, H II 38 and R14—actually appear to be similar to normal Galactic globular clusters.

Another striking difference in Figure 3 between the spectra of M31, Galactic, and M33 clusters is that the M33 clusters have an enormous range in $\text{H}\beta$, presumably due to the large range in their ages. This phenomenon has been observed in the spectra of LMC clusters, as shown by Rabin (1982) and others. To first order, it is reasonable to expect that the $\text{H}\beta$ equivalent width is a fairly reliable (relative) age indicator for clusters younger than 10^{10} yr, but older clusters may contain horizontal-branch stars, which could confound a calibration at low $\text{H}\beta$. The $\text{H}\beta$ equivalent widths of the M33

clusters do correlate with the age estimates derived from the visual examination of the spectra and serve to rank order the clusters, as in Table 3. A precise age calibration of $\text{H}\beta$ depends upon the metallicities and stellar components of the clusters; nonetheless, considering the small range in Mg II values for the clusters, a crude linear relation was derived for $\log(\text{age})$ as a function of $\text{H}\beta$. The very approximate ages, based on $\text{H}\beta$ strength, appear in the last column of Table 3.

In a related discussion, Rabin (1982) argued that atomic lines can enhance the $\text{H}\beta$ equivalent widths in older populations, when measured according to BFGK's prescription. Following a suggestion by S. Faber, E. Friel, and C. Morea (private communication), our $\text{H}\beta$ measurements were examined for such effects. If, for example, both $\text{H}\beta$ and $(B-V)$ are correlated with integrated spectral type (and hence age), a plot of $\text{H}\beta$ versus $(B-V)$ could be calibrated to measure the amount of contamination in the $\text{H}\beta$ value due to strong atomic lines. In Figure 4 are plotted the loci of Galactic cluster sequences with "known" metallicities. Considering objects with $(B-V) > 0.6$ mag, for which this discussion is pertinent, the scatter in the data overwhelms any abundance effects when $[\text{Fe}/\text{H}] > -1.2$, including the M3 data. Only in the extreme case of M15 is there evidence that the $\text{H}\beta$ line strength exhibits metallicity effects; i.e., the $\text{H}\beta$ line strengths for the M15 stars can be considered "metal-contamination free." Figure 4 suggests that the level of contamination in

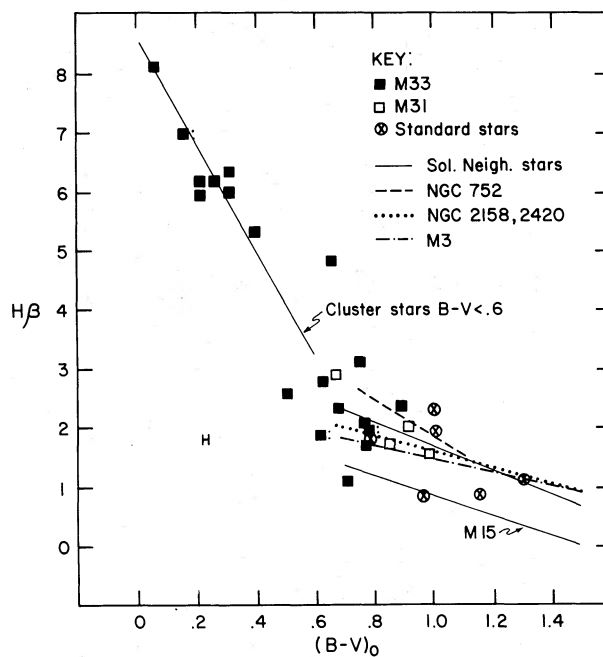


FIG. 4.— $\text{H}\beta$ vs. $(B-V)_0$. The positions of solar-neighborhood field and cluster stars are indicated as solid lines. The loci of evolved stars in clusters of decreasing metallicity are shown also. The figure suggests that the contamination due to metals in the wings of $\text{H}\beta$ is difficult to qualify especially for $[\text{Fe}/\text{H}] > -1.2$ and $(B-V) > 0.6$ mag.

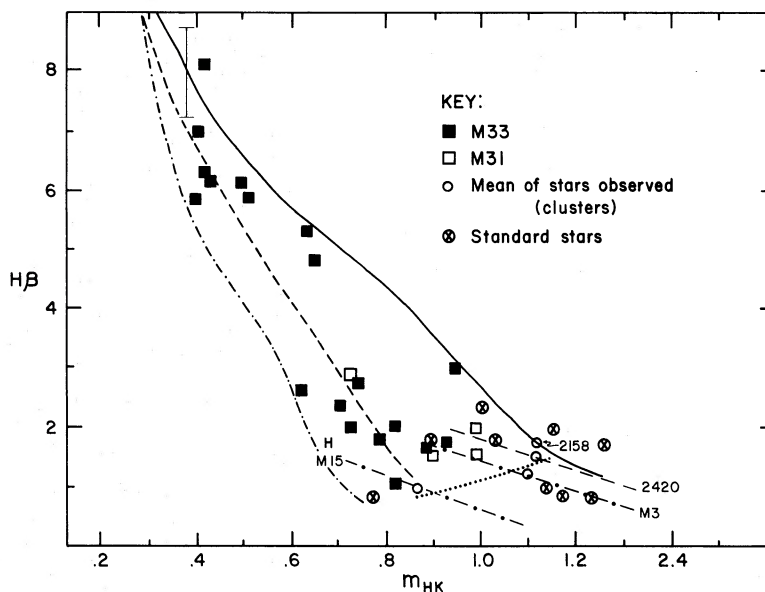


FIG. 5.— $H\beta$ vs. m_{HK} . Indices computed from model spectra are shown as dot-dashed ($[Fe/H] = -2.0$) and dashed ($[Fe/H] = -1.0$) lines. The solid line represents the mean locus of the data from observed solar-neighborhood stars. Data for individual stars in M15, M3, and NGC 2420 scatter around the sequences indicated in the lower portion of the figure. The open circles represent the mean data point for each cluster; these points are joined by the dotted line.

the $H\beta$ equivalent width due to the presence of atomic lines is less than the amount of scatter in our data for $[Fe/H] > -1.2$ and $B-V > 0.7$ mag, so corrections to the ages determined from $H\beta$ are inappropriate for our data. Note that the cluster H II 21 may have either an excessively strong $H\beta$ or a particularly red ($B-V$), possibly due to the presence of luminous evolved stars or contamination by reddening.

c) $H\beta$ versus m_{HK}

Rabin (1982) discussed a diagnostic for determining the age-metallicity relationship for a population of clusters, in particular, as applied to Magellanic Cloud clusters. Two of the parameters Rabin used are the combined equivalent widths of $H\beta$, $H\gamma$, and $H\delta$ and the equivalent width of the Ca II K line. Smith (1980) and Christian and Smith (1983) have described a similar procedure for estimating the metallicities of early-type supergiants, presumably freed from age effects. Regarding the M33 clusters, the two pertinent measurements are $H\beta$ and m_{HK} . Figure 5, analogous to Rabin's Figure 4, displays the relationship between these two parameters for our data set, including the indices computed from the model spectra and sequences derived from individual members of clusters in the Galaxy. The error bars shown indicate the scatter in the observed values for solar-neighborhood stars and the uncertainty in the $H\beta$ values for the model indices. The dotted line joins the mean data points for NGC 2420, M3, and M15, representing the locus of late-type giants with differing metallicities.

The distribution of M33 clusters is superficially similar to that of the LMC clusters observed by Rabin.

However, the M33 clusters span the entire range of $H\beta$ values and extend up to the region occupied by early-type solar-neighborhood stars. The former comment was expected from Paper I and discussions above, where it was shown that the M33 cluster population includes luminous objects covering a wide range of ages, traced by $H\beta$. The second observation is in contrast to what is found for the LMC, where the integrated cluster and color-magnitude diagrams suggest that the youngest LMC clusters in Rabin's sample (these are not the youngest objects in the LMC, however) are metal-poor with respect to the Sun (Rabin 1982; Cohen 1982, and references therein).

At this point it is important to recognize the differences between Suntzeff's m_{HK} index and the Ca II line measurements discussed in the above references. The K line indices and equivalent widths, designed to measure early-type spectra, reflect basically the strength of only the Ca II K feature. At a given spectral type, say F2, the Ca II K line is enhanced in high-luminosity stars, while the hydrogen line strengths are diminished. Thus, the equivalent width of the Ca II K line increases with increasing luminosity. However, the m_{HK} index, designed for late-type stars, decreases, causing higher luminosity stars to overlap with lower metallicity stars in the m_{HK} versus ($B-V$) plane. Luckily, in the $H\beta$ versus m_{HK} plane both indices decrease for high-luminosity stars; the result is that class V and I stars define the same sequence, to within our measuring accuracy, for $3.0 < H\beta < 7.5$, at a given metallicity. This result, which allows a deconvolution of age and abundance for the blue M33 clusters, was verified by

examining the data for individual early-type stars. The clusters U62, M4, M6, U83, and H II 21, which lie close to the solid line in the figure, should have roughly solar metallicity, and U101, Cl 27, and U79 may be slightly metal-poor. The precise values of the cluster abundances obviously depend upon the accuracy of model indices and the amount of extinction in each object.

In the redder, older clusters, evolved stars and often BHB stars are the basic constituents, with some contribution from main-sequence and turnoff stars, making the deconvolution of age and metallicity troublesome. With the exception of Cl 18, Cl 20, and Cl 39, the red M33 clusters follow a smooth distribution from the $[\text{Fe}/\text{H}] = -1.0$ sequence to the region occupied by globular clusters. At $H\beta \sim 2.5$, Cl 18 and Cl 39 have the most extreme values of m_{HK} ; Cl 18 exhibits a nearly solar value, while Cl 39 has a weak H and K feature. Cl 20 may have weak line indices due to metallicity effects coupled to weakening due to poorer signal-to-noise ratio in the observed spectrum.

d) CN $\lambda 4170$ versus Mg II

Borson (1982) has discussed a method for deconvolving the integrated spectral features of galaxies, using the strength of CN (4216 or 3880 band) in comparison to the Mg $\lambda 5175$ line strength. In the CN versus Mg plane, as for other indices, the location of a particular object should be a function of abundance and age, or at least the temperatures of the constituent stars. To facilitate comparison between our data, BFGK, and Borson, the CN $\lambda 4170$ index and Mg II indices were used to examine the M33 data set. Note that Mg II is almost identical to Borson's Mg b index.

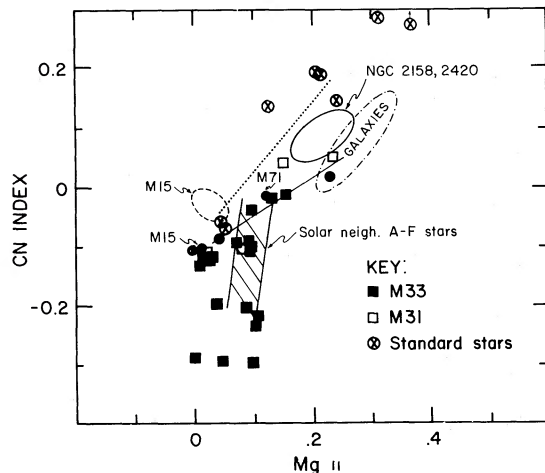


FIG. 6.—CN $\lambda 4170$ vs. Mg II. The dotted line connects the solar-neighborhood giants' data to metal-poor evolved stars. The cross-hatched region indicates the position of indices from early-type stars and model spectra. The solid line connects Galactic globular clusters to the galactic nuclei measurements; the unlabeled filled circles represent M92, M3, and M32 (from BFGK) in order of increasing Mg II.

Figure 6 displays the computed indices for M33 and M31 clusters and comparison objects.

The dotted line in the figure joins the indices of solar-abundance giants to the locus of the metal-poor giants, which include M15 stars and the two metal-poor standards. The line delineates the region occupied by stars with the same broad-band colors and approximately the same luminosity. Scatter away from the line is caused by variation in luminosity and $[\text{CN}/\text{Mg}]$, and positions along the line should reflect abundance. The solid line connects the integrated indices for Galactic globular clusters to the values for galactic nuclei (from BFGK). The crosshatched region shows the locus of the observed early-type stars; the indices computed for the model spectra, which show only slight variation with $[\text{Fe}/\text{H}]$, fall in this region also.

At lower abundances ($\text{Mg II} < 0.12$), the integrated indices of some clusters exhibit a large decrease in CN $\lambda 4170$, when compared with the spectra of individual stars. In § Vb, it was demonstrated that the presence of hot stars in lower abundance objects does not appreciably affect the integrated Mg II index, suggesting that a relative weakening of the CN $\lambda 4170$ feature can occur independently of variations in the Mg line strength. As an example, for M15, the data for both individual giants and the integrated spectrum are available, and indicated in Figure 6. The simultaneous increase in the integrated $H\beta$ value, independent of Mg II (see § Vc), provides further supporting evidence for this conjecture. In spectra of objects with $\text{Mg II} > 0.2$, the variation in CN $\lambda 4170$ is complicated by luminosity effects, since high-luminosity, high-metallicity red stars have strong CN features. Fortunately for our purposes, the M33 clusters all have $\text{Mg II} < 0.16$.

In this figure, Cl 36, H II 38, and R12 seem to be examples of bona fide globular clusters, extending up to the region near M71. R14 and M9 have Mg II indices similar to M3 but show a slight weakening in CN index. Many of the remaining clusters appear to contain a strong blue stellar component, causing a substantial weakening in CN $\lambda 4170$, and these clusters also exhibit enhancements in $H\beta$.

e) Discussion

In the spectral range 3600–5400 Å, the spectrophotometry indicates that the M33 cluster population exhibits a wide range of ages, from 10^7 to 10^{10} yr. The cluster metallicities seem to follow smoothly with the ages, in general, but do not fall below $[\text{Fe}/\text{H}] = -2.0$. Individual clusters show some interesting features which often deviate from the general rule. None of the clusters exhibit extremely enhanced CN features. Also, our spectrum of the M31 cluster 171-222 (called V87 in BFGK) does not exhibit an abnormally strong CN $\lambda 4170$ feature, relative to its Mg II index. A summary of the characteristics of each cluster observed is presented in Table 4, where importance has been placed on the cumulative information derived from the spectra. In the second through fourth columns, the headings refer to the figures discussed above.

TABLE 4
SUMMARY OF CLUSTER CHARACTERISTICS

Cluster	m_{HK} vs. ($B-V$)	H β vs. Mg II	H β vs. m_{HK}	CN vs. Mg II	Comment
U62	a	a	a	b	Young, solar abund.
U148	a	a	a, c, d	b	Young, solar abund., + high- L stars
M4	a	a, b, c	a, b, c	e	Young, < solar abund.
M6	a	a, b, c	a, b, c	e	Young, < solar abund., + O stars
U79	a, d	a, b, c	a	b	Young, < solar abund., + high- L stars
Cl 27	c, d	d	c	b	O III emission, + high- L stars
U101	c, d	d	c	b	Slightly metal-poor, + high- L stars
U83	a, d	d	a	b	< solar abund., + high- L stars
Cl 39	c, d	f	c	e	Metal-poor, intermediate age
H II 21	c, d, g	g, h	a, b, c	a?	Strong H lines, solar abund., + high- L red stars
U49	c, d	h/i	j	k, b	High- L stars, possibly some late-type (enhanced H, Mg II)
R14	f	f	j	k, b	Globular?, intermediate abund., [Fe/H] ~ -1.2
M9	f	f	j	k, b	Globular?, intermediate abund., [Fe/H] ~ -1.2
Cl 18	a, l	h	h, l	e	g band, H β , m_{HK} strong (BHB or turnoff stars?)
Cl 38	f	f	j	e	Intermediate age to globular, intermediate abund.
Cl 20	c, f	c, f	c	k, b	Signal-to-noise ratio + metal-poor?
R12	f	i	j	m	Metal-rich globular, g band, CN bands (3883) strong
H II 38	f	i	j	k, b	Metal-rich globular, g band, CN bands (3883) strong
Cl 36	g	i	j	m	Intermediate age + high- L red stars

^a Near solar metallicity sequence.

^b Weak CN.

^c Near low-metallicity sequences ([Fe/H] = -1.0, -2.0).

^d May have high- L evolved stars.

^e Near M15.

^f Near globular cluster sequence.

^g Unusually red ($B-V$) for corresponding index.

^h Strong H β .

ⁱ Strong Mg II.

^j Within smooth distribution extending to globular sequence.

^k Near intermediate position on globular sequence.

^l Strong m_{HK} .

^m Near M71.

VI. SUMMARY

Integrated IIDS spectrophotometry has been obtained to examine the distribution of ages and metallicities of 20 M33 clusters in relation to clusters in other Local Group galaxies. Based on a comparison with integrated spectra of M31 and MC clusters, spectrophotometric indices of field stars, model spectra, and individual cluster members, we draw the following conclusions:

1. The M33 clusters observed span a wide range of ages (10^7 – 10^{10} yr) and metallicities ($-2.0 < [\text{Fe}/\text{H}] < 0.0$).

2. The spectral type and age ranking of the clusters are well correlated with integrated ($B-V$) and the

equivalent width of H β ; therefore, the clusters sampled do not suffer from strong reddening within M33.

3. The reddest, presumably oldest clusters, H II 38, Racine 12, Racine 14, Cl 36, and possibly Cl 20 exhibit line indices characteristic of the "true" globular clusters found in the Galaxy. These objects range in abundance from that of M71 down to, but not less than, that of M15. None of the clusters in M33 appear to be as metal-rich as the strong-featured, bright clusters in M31.

4. The bluest, young clusters appear to be metal-rich. The precise range and overall age-metallicity relations are difficult to deconvolve without performing a detailed population synthesis, which is beyond the scope of this survey. Nevertheless, excluding Cl 39

and Cl 18, the age-metallicity relation actually may be relatively simple; i.e., clusters with ages from 10^7 to 10^{10} yr have abundances varying smoothly from $[\text{Fe}/\text{H}] \sim 0.0$ to ~ -2.0 . In this respect, M33 appears to be a galaxy intermediate between the Galaxy and the LMC.

5. None of the clusters exhibit unusually strong CN features for their Mg II indices, including M31 171-222, an object for which BFGK measured a strong CN $\lambda 4170$ feature.

A preliminary investigation of the M33 cluster system (Christian and Schommer 1983) found that the velocities of some of the blue clusters appear kinematically similar to the H I disk, while the reddest clusters have non-disklike motions. Further analysis of the velocities of these and additional M33 clusters is in progress and offers the interesting possibility of correlating the ages, abundances, and kinematics of the cluster system in another galaxy. This opportunity allows us to explore the history of star formation and chemical enrichment in M33. With a sizable sample of cluster velocities it also is possible to examine kinematics in the context of ages of stellar populations, yielding information about rapid collapse of disk systems, a much debated point with regard to our own Galaxy.

The use of $\sim 10 \text{ \AA}$ resolution spectrophotometry has proven to be a powerful tool for intercomparison of integrated spectrophotometry of clusters, galactic bulges, and galactic nuclei. In the case of the M33 data, we

were able to verify the existence of young, luminous, relatively massive clusters as well as older, more classical globular clusters in M33. As suggested in Paper I, it seems that the conditions for star formation in M33 have been relatively stable and conducive to the production of massive clusters during all epochs. In other Local Group galaxies this has not been the case; for example, in the Galaxy, it is possible that massive clusters were produced in the halo only. In the Magellanic Clouds, massive young clusters have formed recently, but the star formation rate there appears to be more "bursty" (Rabin 1982; Aaronson and Mould 1982). It should be kept in mind, however, that although the luminosities of the younger M33 clusters indicate they are more massive than typical Galactic open clusters, the *most* massive clusters discovered in *all* galaxies are the oldest objects, i.e., the globular clusters. Finally, note that a more precise description of the age-metallicity relation and intrinsic scatter for M33 clusters will be attempted upon the acquisition of a larger data base.

The authors would like to acknowledge the advice and helpful discussions of Drs. D. Burstein, N. Suntzeff, S. Faber, R. Kraft, and Ms. E. Friel. We wish to thank Drs. S. Faber, C. Morea, and Ms. E. Friel specifically for providing us with data in advance of publication. Finally, we express our gratitude to the KPNO TAC for the allocation and conscientious scheduling of our telescope time.

REFERENCES

- Aaronson, M., and Mould, J. 1982, *Ap. J. Suppl.*, **48**, 161.
 Battistini, P., Bonoli, F., Braccisi, A., Fusi Pecci, F., Malagnini, M. L., and Marano, B. 1980, *Astr. Ap. Suppl.*, **42**, 357.
 Boroson, T. 1982, preprint.
 Burstein, D., Faber, S., Gaskell, C. M., and Krumm, N. 1982, in *IAU Colloquium 68, Astrophysical Parameters for Globular Clusters*, ed. A. G. D. Philip and D. S. Hayes (Schenectady, N. Y.: L. Davis Press), p. 441 (BFGK).
 Canterna, R., Harris, W. E., and Farrell, T. 1982, *Ap. J.*, **258**, 612.
 Christian, C. A. 1981, *Ap. J.*, **246**, 847.
 Christian, C. A., and Schommer, R. A. 1982, *Ap. J. Suppl.*, **49**, 405 (Paper I).
 ———. 1983, in *IAU Symposium 100, Internal Kinematics and Dynamics of Galaxies*, ed. E. Athanassoula (in press).
 Christian, C. A., and Smith, H. A. 1983, *Pub. A.S.P.*, **95**, in press.
 Cohen, J. 1982, in *IAU Colloquium 68, Astrophysical Parameters in Globular Clusters*, ed. A. G. D. Philip and D. S. Hayes (Schenectady, N. Y.: L. Davis Press), p. 229.
 Faber, S., Friel, E., and Morea, C. 1982, preprint.
 Gunn, J. E., Stryker, L. L., and Tinsley, B. M. 1981, *Ap. J.*, **249**, 48.
 Gustafsson, B., and Bell, R. A. 1978, *Astr. Ap. Suppl.*, **34**, 229.
 Harris, W. E., and Racine, R. 1979, *Ann. Rev. Astr. Ap.*, **17**, 241.
 Hiltner, W. 1960, *Ap. J.*, **131**, 163.
 Kinman, T., Kraft, R., and Suntzeff, N. 1981, in *Physical Processes in Red Giants*, ed. I. Iben and A. Renzini (Dordrecht: Reidel), p. 71.
 Kron, G., and Mayall, N. 1960, *A.J.*, **65**, 581.
 Kurucz, R. L. 1979, *Ap. J. Suppl.*, **40**, 1.
 McClure, R. D., and Hesser, J. E. 1981, *Ap. J.*, **246**, 136.
 O'Connell, R. 1982, *Ap. J.*, **257**, 89.
 Pritchett, C. 1977, *Ap. J. Suppl.*, **35**, 397.
 Rabin, D. 1982, *Ap. J.*, **261**, 85.
 Sargent, W. L. W., Kowal, S. T., Hartwick, F. D. A., and van den Bergh, S. 1977, *A.J.*, **82**, 947.
 Smith, H. A. 1980, *A.J.*, **85**, 848.
 Strom, K. 1977, *Standard Stars for IIDS Observations* (Tucson, Ariz.: Kitt Peak National Observatory).
 Suntzeff, N. 1980, *A.J.*, **85**, 408.

Note added in proof.—The photometry for Cl 27 was misquoted in Paper I. Hiltner's values are $V = 17.1$, $B - V = 0.4$.

CAROL A. CHRISTIAN: Canada-France-Hawaii Telescope Corporation, P.O. Box 1597, Kamuela, HI 96743

ROBERT A. SCHOMMER: Rutgers University, Department of Physics and Astronomy, P.O. Box 849, Piscataway, NJ 08854